Application of Silicon Photomultipliers in Scintillation based radiation detectors

Contact: ad16020@bristol.ac.uk

A.Dasgupta
School of Physics,
University of Bristol,
BS8 1TH, United Kingdom

M. Sperrin, A Hallman
Department of Medical Physics and Clinical Engineering, Churchill Hospital, Oxford
OX3 7LE, United Kingdom

J. Matheson
Department of Particle Physics,
Science and Technology Facilities Council,
Rutherford Appleton Laboratory

C.D. Armstrong,
R. Heathcote, R.Clarke,
G. McBride, D. Neely
Central Laser Facility,
Science and Technology Facilities Council,
Rutherford Appleton Laboratory

Abstract

An application for Silicon photomultipliers as sensitive time resolved radiation detectors was investigated. Absolute light responses, with and without amplification was investigated, for different models of SiPMs. Radiation spectra with LYSO were also obtained. It was found that in terms of sensitivity, the SiPMs with the set-up used were able to produce readouts in the order of 10s of photons, but require amplification to approach this level.

1 Introduction

Scintillation based detectors are commonly used to measure radiation levels and extract spectral information. Radiation incident on a scintillator will deposit some energy into it, which can be re-emitted as light at a longer wavelength. For many radiation sources this emission often approaches the single photon level.

Silicon photomultipliers (SiPM) are photon sensitive detectors, comprised of avalanche diode arrays implemented in a silicon substrate. They are advantageous over the traditional photo multiplier tubes in that they are lower in cost, more robust and smaller in form (typically only a few millivoltmeters). Their sensitivity allows them to be used as photodiodes for measuring low intensity short pulses of scintillation light. This report seeks to characterise these devices for use as a radiation detector. This report primarily focuses on the performance of KETEK PM3315-WB and PM3325-WB SiPMs, comparing them to a more expensive SensL chip, and examining their use in a LYSO based scintillation detector.

2 SiPM tests

SiPMs are composed of many 'microcells', which are couplings of a silicon photo-diode and a resistor, in reverse bias (Fig. 1). Light incident onto the diode can be absorbed by an electron, which will be accelerated towards the cathode, gaining enough kinetic energy to create further charge carriers by impact ionisation. This avalanche causes the silicon to break down, and causes a macroscopic current to flow freely through it, until the potential drop across the resistor quenches it.

The SiPM being tested is the KETEK 3×3mm WB series chip. This comes in two variants, one with a microcell size of 25μm, and one with 15μm. Having the same area means the larger cell size chip has fewer microcells. A comparison of these to a 6×6mm SensL chip is found in Table (1).

	KETEK PM3315 -WB	KETEK PM3325 -WB	SENSL MICRO-FJ 600035-TSV
Active Area (mm^2)	3.0×3.0	3.0×3.0	6.07×6.07
Microcell size (μm)	15	25	35
Number of microcells	38800	13920	22292

Table 1: Comparison of the KETEK WB series SiMP with the SensL FJ series SiMP [1–3]

3 Methods

In characterising the SiPMs, a few aspects were considered. To estimate the amount of light (number of photons) incident on the chip from the measured output, the device must be calibrated absolutely. Secondly, the peak output of the SiPM is known to be generally non-linear, but for low photon flux it may be approximated as linearly (see Sec.5). At high fluxes the output of the SiPM approaches a saturation limit as all the cells are

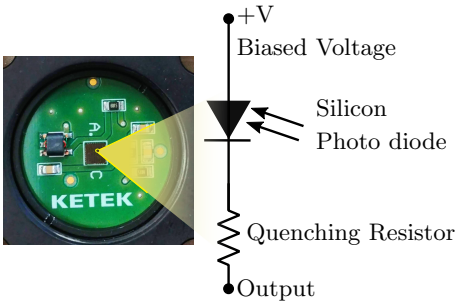

Figure 1: Picture of KETEK SiPM chip, integrated into a PCB, with a schematic of a micro cell

discharged, and hence it is favourable to operate in the linear response region. This linearity was investigated, as well as what parameters may be tuned to maximise linearity.

Secondly, the SiPMs intrinsically have an associated 'recovery time' after each detection, which is the time taken for the reverse bias across the photodiode in each cell to be re-established. In the output this is seen as a sharp rising edge, as the breakdown occurs and current flows, followed by an exponential like decay as the current is quenched. The effect of this in the time resolution of the device was tested.

Finally, in order to demonstrate the SiPMs working as radiation detectors, the spectrum of a radioactive source was reproduced.

3.1 LED characterisation

A short pulse light source is needed to calibrate the SiPMs, both because the type of scintillation light we seek to simulate is short pulse in nature, and because the SiPMs cannot operate well in long pulse / CW settings. An LED was used as the light source. Primarily a 405 nm LED was used through the tests, as its wavelength closely matches the 420 nm emission of the LYSO scintillation, but other wavelengths were also used when comparing the different brands of SiPM, the exact emission spectra of which are found in Fig.2.

A 40 ns pulse was driven through the LED. To estimate the number of photons incident from the LED, a calibrated photodiode (Thorlabs S120VC) was used to measure the power incident from the LED at the distance the SiPMs would be placed. The solid angle subtended by the collection aperture of the photodiode is comparable to that of the SiPM, so the power incident was assumed to be directly proportional to area between the two. While the power deposited by a 40 ns pulse is too low for the power meter to detect, if the LED is driven at a high repetition rate then the average power is detectable. The energy per pulse in the equivalent solid angle is the measured power divided by the driving frequency.

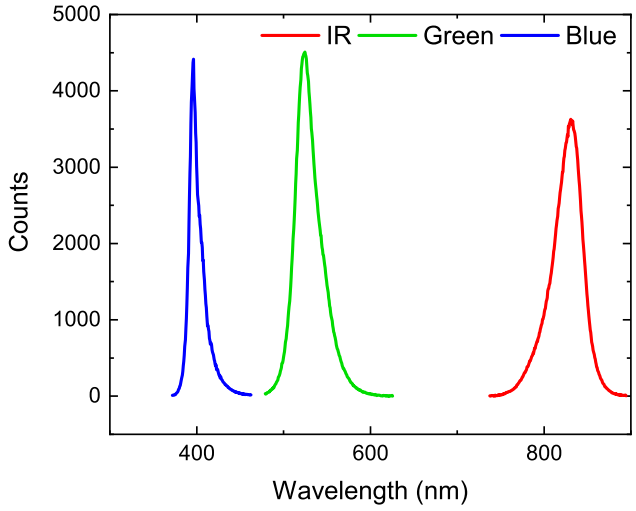

Figure 2: The emission spectra of the 3 LEDs used in these tests, as measured using an Avantas spectrometer. These are labelled 'IR', 'Green' and 'Blue', and will be referred to as such through the report

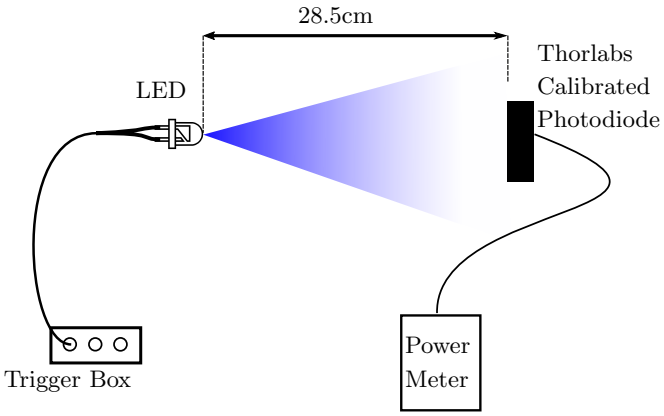

Figure 3: Setup for determining the number of photons delivered from the LED to the SiPM. A factory calibrated photodiode is placed in place of the SiPM. The LED, pulsing at 40ns, is driven at a high repetition rate (kHz), so that the average photon flux is detectable by the photodiode.

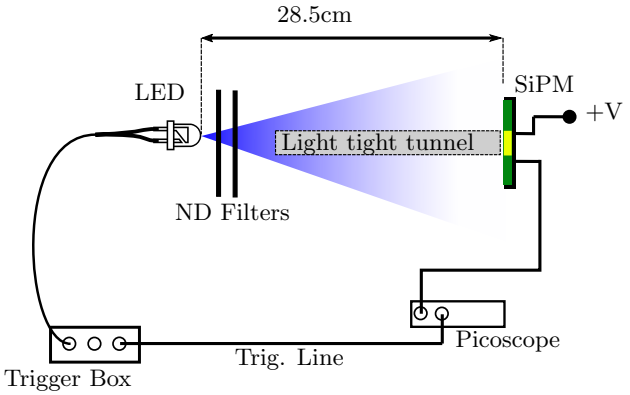

Figure 4: Setup for SiPM LED response test. The LED is pulsed at 40ns, via the trigger box, which at the same time sends a trigger to the Picoscope to begin acquiring. The SiPM is placed in line with the LED, with ND filters between them to control the number of photons incident. A light tight tunnel ensures no scattered light falls on the detector face. The bias voltage is controlled by a bench power supply.

Having determined the number of photons incident from the LED on the SiPM, the number of photons were controlled by placing Neutral Density (ND) filters between the LED and the SiPM (Fig. 4). The method is adapted from a camera calibration carried out by Rusby[4]. in this way the SiPMs were subjected to progressively lower levels of light, with their output measured.

The SiPM face was encased in a light tunnel to stop diffracted LED light from falling on the sensor. The output of the SiPM was digitised using a Picoscope 6404D, at 50Ω coupling. The SensL and the KETEK (15μm cell size) SiPMs were tested with the 3 different LEDs at 30V bias voltage to compare their responses. The two KETEK SiPMs were then tested with a more gradual increment of ND filters, at different biased voltages to examine the effect of operating voltage on linearity.

3.1 Choosing Oscilloscope coupling

The Picoscope used allowed for the input of the SiPM to be coupled either to a 1MΩ ('DC') or a 50Ω input. It was found that the DC coupling, while having a greater peak voltage, causes an impedance mismatched ringing effect on the SiPM output, and so the 50Ω coupling was chosen.

3.2 Acquiring spectra

A spectrum from an actual radiation source was also obtained using both the KETEK SiPMS. The radiation source was ^{22}Na, which emits at a characteristic 511 keV. The full width half max of the measured 511 keV peak is taken to be the energy resolution of the SiPM. The

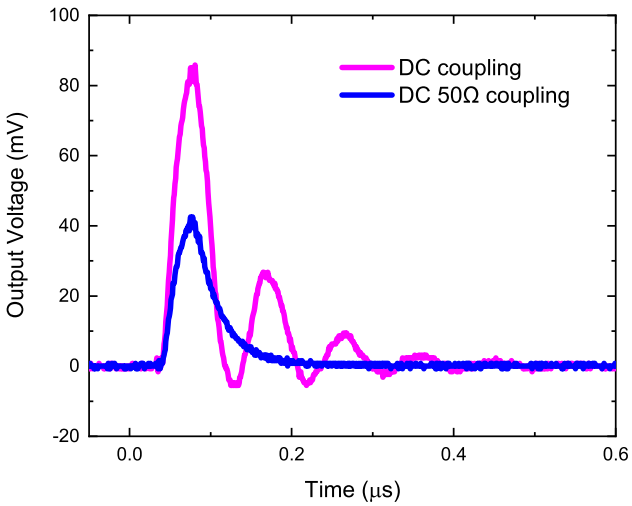

Figure 5: The same pulse (SiPM detecting LED flash) on a DC and 50Ω coupling. The 50Ω was chosen for the tests carried out.

SiPMs were sequentially coupled to the same LYSO crystal for this test (Fig. 6).

3.2 Choosing Scintillator

The SiPM becomes a radiation detector when coupled to a scintillator. These are materials which absorb incident radiation, and re-emit it at a lower energy (typically optical light). The scintillator chosen was LYSO (Lutetium-yttrium oxyorthosilicate). For the chosen scintillator, the parameters of interest are decay time and light yield. Decay time indicates the speed of the scintillation, becoming a limiting factor to time resolution, while greater light yield in terms of photons per MeV of energy deposited leads to a bigger signal. The density and attenuation coefficient must also be taken into consideration. These determines how much energy of an incident beam is actually deposited into the material. For the radiation detectors this report seeks to characterise, a balance between speed and signal must be struck. Comparing some common scintillators (Fig.8) [5] show that LYSO strikes the best balance in terms of speed and light yield.

A notable disadvantage of LYSO is its self emission. 23% of Lutetium is radioactive, and this leads to LYSO emitting radiation which can be self absorbed, leading to a baseline glow. This is not a significant problem for smaller sized crystals, but for larger crystals the effect may be limiting to the detection threshold of incident signals.

3.3 LED pulse pile up

Finally, the time resolution,(the ability to resolve 2 consecutive pulses separated in time) was tested on the 15μm KETEK sensor. The same set-up as Fig. 2 was

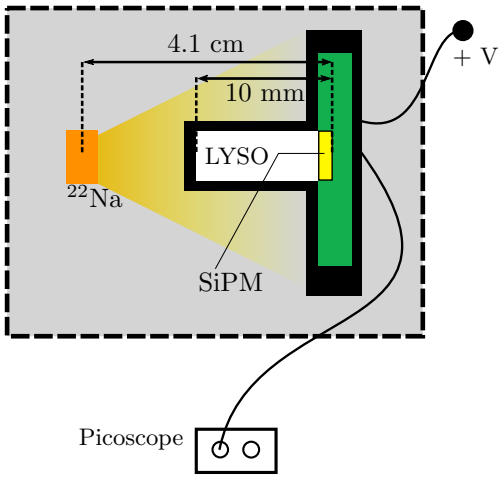

Figure 6: Setup for acquiring the 511 keV emission spectrum. The radioactive source used was a ^{22}Na. The SiPMs were coupled to a 2x2x10mm LYSO crystal,and placed in line with the radiation source. A biased voltage of 30V was used. The Picoscope was set to 50Ω coupling

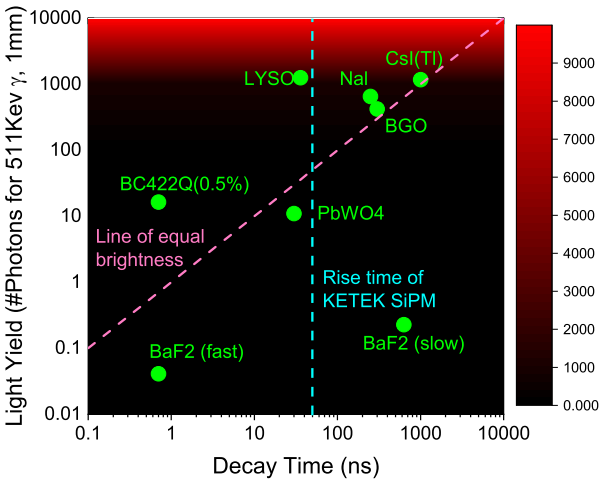

Figure 7: Decay time to Light yield of different scintillators. Light yield calculated from manufacturer quoted photons per MeV, densities, mass attenuation coefficients from the NIST database. Calculated for 1mm of material, for an incident 511 keV incident emission

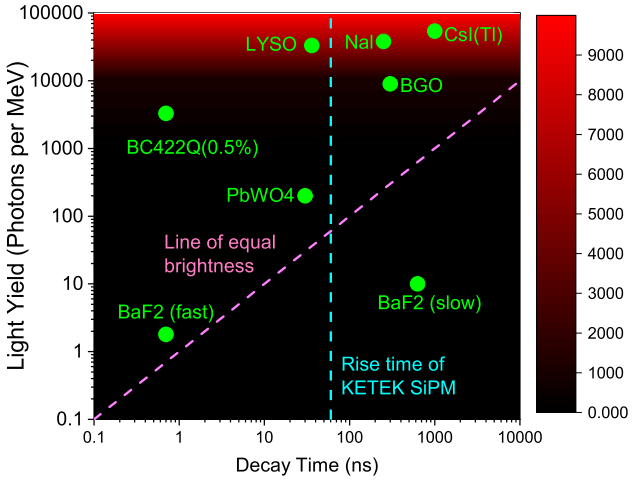

Figure 8: Decay time to Light yield of different scintillators, in terms of photons per MeV, and not accounting for difference in density and atomic cross section.

used, except with 2 LEDs, with firing time controlled using the trigger box. Intending to implement this sensor coupled with LYSO, the pulses were tuned to simulate the LYSO emission. They were 68ns in width, and ND filters were used to adjust the peak height to around 14 mV, representative of a typical 511 keV LYSO emission (Fig. 15). The LEDs were pulsed with some separation between them, with this time progressively stepped down.

4 Comparing SiPM brands

The KETEK 15μm and SensL chips were directly compared to each other in terms of their response to different intensities of light. The KETEK chips are more cost effective and therefore flexible to use. They were subjected to varying level of light as described in Sec. 3.1, with all three of the available LEDs. This gave a comparison of sensitivity across the three wavelengths. As this test was comparative the ND filter increment was relatively coarse, increments of ND 0.5 was used as opposed to the 0.2 in later tests. With the setup used it was found that the noise floor was about 2mV, so signals lower than that were not readily detectable.

The SensL sensor was found to be an order of magnitude more sensitive than the 15μm KETEK sensor. A significant contributor to this is the larger cell size of the SensL chips (Table.1). Larger cells hold more electrons in the P-N junction of the photodiode, and so each cell fires with a greater gain. This is seen later when comparing the 2 KETEK chips to each other. Looking only at the Blue LED response, cell size and gain seem to be correlated (Fig.10). The exact relationship between the area of each cell and gain was difficult to empirically demonstrate here with limited data points and different brands of SiPM, but the takeaway is the greater sensitiv-

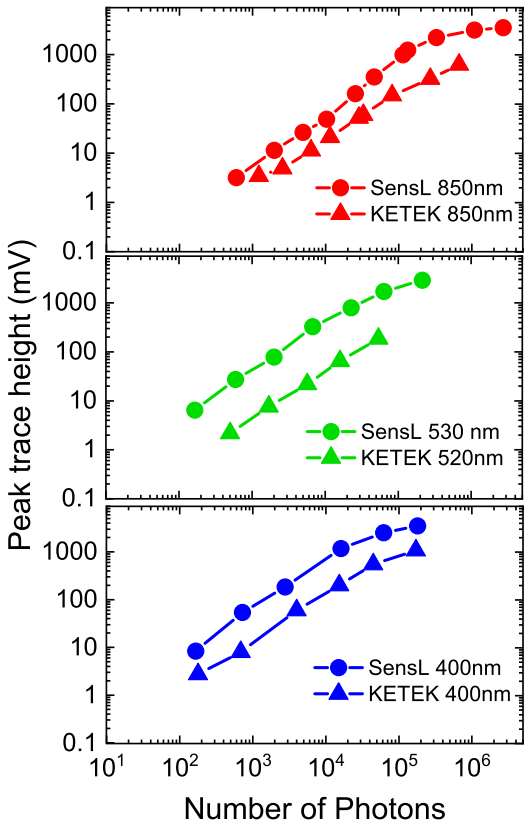

Figure 9: Photon response of the KETEK and SensL SiPMs at 30V Biased voltage, for the IR (left), Green (center) and blue (right) LEDs. The Peak wavelengths are indicated. The SensL chip is consistently more sensitive, in large part due to the larger cell area

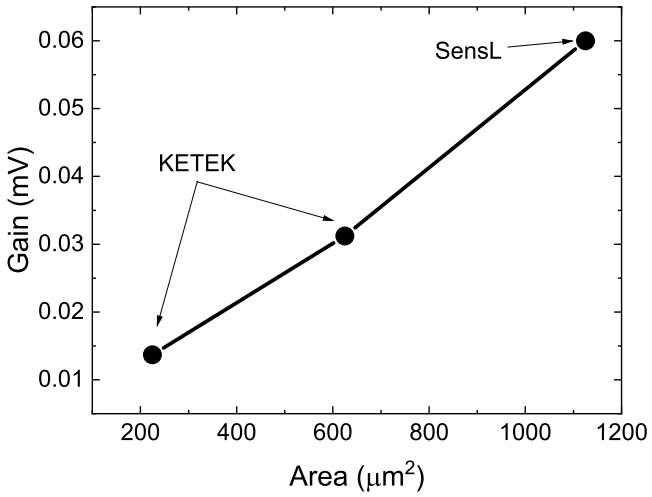

Figure 10: Cell area and effective gain in linear region (see section 5) for the three chips tested, with the blue LED at 30V biased voltage.

ity of the SensL chips may be to a large part attributed to a greater cell size.

When tested with the LED it was found that the disparity is greatest for the Green LED where the SensL sensor was an order of magnitude more sensitive than the KETEK(Fig. 9). For the IR LED the curves are comparable, and for Blue, the wavelength similar to the emission of LYSO, the Sensl was approximately 3 times as sensitive. The response for both sensors are aproximately linear, becoming more non linear with high photon flux (See Sec. 5).

5 Linearity, Gain and Efficiency

In order to use the KETEK sensors it is important to determine both what the expected peak voltage is for a given number of photons incident, and to what extent this response is linear for both cell sizes.

Once a photon causes a cell to fire, that particular cell becomes depleted and unable to fire again for a short time, and so for the next photon incident in that timescale there are fewer cells available to detect it. Let N_c be the number of micro cells in a SiPM. A statical analysis shows that for N_p incident photons, the number of cells that fire is given by [3]:

$$N_{fired} = N_c\left(1 - \exp\left(\frac{\epsilon(V_{bias}, \lambda)N_P}{N_c}\right)\right) \qquad (1)$$

Where ϵ is the detector efficiency. ϵ is a function of bias voltage and wavelength, and represents the combined influence which is dependent on many effects. In terms of the peak voltage measure, V_{peak}, we must consider the contribution to the peak voltage made by each cell fired, which we define as gain (g), and which is also a function of biased voltage:

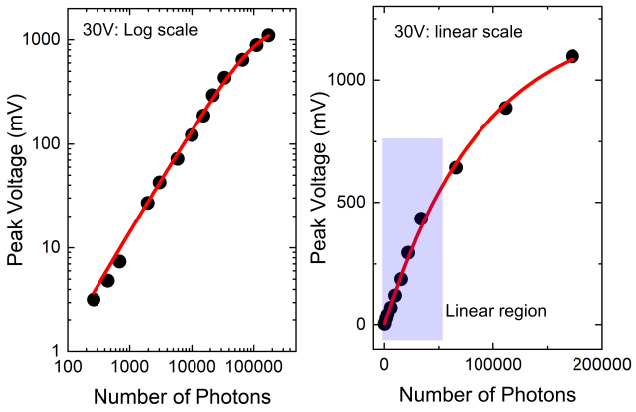

Figure 11: Example of fitting Eq.2 to light response (Blue LED, 30V biased voltage shown). As can be seen, the fit agrees with the the points well, with R-squared values of unity to 2 decimal places.

$$V_{out} = g(V_{bias})N_c\left(1 - \exp\left(\frac{\epsilon((V_{bias},\lambda)N_P}{N_c}\right)\right) \quad (2)$$

Expanding this we see that the equation is linear to the 1st order, and the peak voltage is directly proportional to N_P:

$$V_{out} = (g\epsilon)N_P + \mathcal{O}\left(\frac{N_p}{N_c}\right)^2 \quad (3)$$

We define here 'linear' to be the region where the 1st non-linear term in the expansion of Eq. 2 contributes to less than 10% of the total.

The KETEK sensors were tested using the blue LED to simulate LYSO emission and a response curve was obtained at different biased voltages for both chips. A fitting of the form in Eq. 2 with fit parameters of ϵ and g was calculated for each biased voltage. The fit was found to agree well with the obtained data (Fig. 11), however, the fit parameter ϵ had significant error. Despite the R^2 value of near unity for most fits, inspection shows that the data points do deviate somewhat from the fitted line. While not by much, since the shape of the curve is very sensitive to the parameter of ϵ, the scatter that is present significantly increases the uncertainty of its value, as seen by the larger error bars. The errors of the g parameter are not as large, as it controls the scale of the curve described in Eq.1. It however will change if ϵ is changed to rescale the graph. Indeed a differently shaped but similarly good R^2 value fit may be devised with a different value of ϵ if the g value is appropriately tweaked. This dependence means an error in ϵ is an error in g.

The point being stressed here is, while in derivation of Eq.2 the parameters of ϵ and g had real world analogues (namely the efficiency and gain respectively), in this report the relationships derived for the parameters g and ϵ DO NOT correspond the the true device efficiency and gain. The fitting of ϵ and g with biased voltage (Fig. 12) shows that for both chips, the gain is linear with biased voltage, while a square root function best describes the shape of the efficiency curves. It is true that gain and efficiency are functions of biased voltage. Higher biased voltage increases the electron energy and hence the magnitude of the avalanche, which is associated with higher gain. It also increases the probability that a promoted electron causes an avalanche at all, which is associated with efficiency. However, the values for ϵ do not follow the manufacturer quoted values, which predicts lower efficiency for both chips, as well as the 15μm cell sized chip being less efficient than the 25μm one.

It is possible the relationship of g and ϵ is a product of the way in which the fitting algorithm optimises the parameters, and the true relationship between gain and efficiency with biased voltage are both non-linear in a more complicated way. However the g and ϵ values along with Eq.2) provide a good approximation for the shape of the response curve. In the linear response region defined in Eq.3), the effective gradient is just $g\epsilon$, so in this region one can use the values obtained for g and ϵ to derive both the extent of the linear region for a given biased voltage, as well as the effective linear gradient of the region. The max number of photons bounding the linear region is when the first non-linear term is small (taken here to be 0.1). Hence:

$$\begin{aligned} \frac{1}{2}\left(\frac{\epsilon N_{p\,max}}{N_c}\right)^2 &= 0.1 \\ \Rightarrow N_{p\,max} &= \frac{\sqrt{0.2}N_c}{\epsilon} \end{aligned} \quad (4)$$

Here we see a trade-off: The gradient in the linear region, which is indicative of sensitivity, is given by ϵg (Eq.3), and since g and ϵ increase with biased voltage, so does the sensitivity. Between the chips it is also evident that a smaller number of physically larger micro cells as in the 25μm celled chip increases sensitivity. However, the size of the linear response region, bounded by $N_{p\,max}$, changes with both N_c and $1/\epsilon$. Hence one can achieve greater sensitivity by both increasing the bias voltage and choosing a larger cell size chip, but both of these reduce the size of the linear response region of the SiPM.

To confirm the validity of the light response model in predicting the gradient and domain of the linear response region of the SiPM chips, a linear fit for the linear appearing parts of the response curves was applied, and its gradient taken as the 'measured' gradient. Using the fit parameters from Fig.12) for the two KETEK chips, and substituting these into Eq.3, a 'Predicted' gradient was obtained. The measured points were found to lie close to the predicted ones (Fig. 13), and comfortably lie in the region of standard error of the model. Note the errors in measurement are higher for the 25μm cell, as

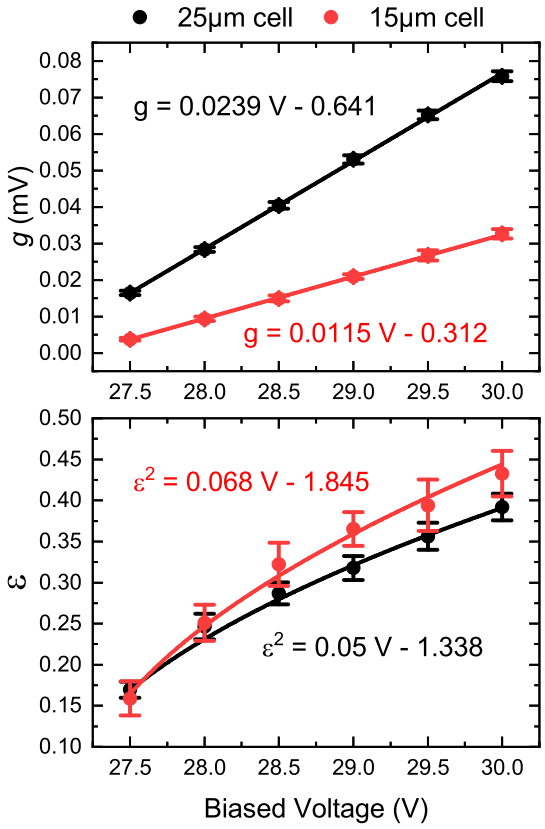

Figure 12: Plot of KETEK SiPMs ϵ (top) and g (bottom) as a function of biased voltage. The plot points are derived from fitting response curves similar to Fig. 11 for both chips at different biased voltages. The g shows a linear relationship with applied voltage, while it is empirically demonstrated that the square of the ϵ varies with the voltage. Tests conducted with the blue LED, and 50Ω coupling on the picoscope.

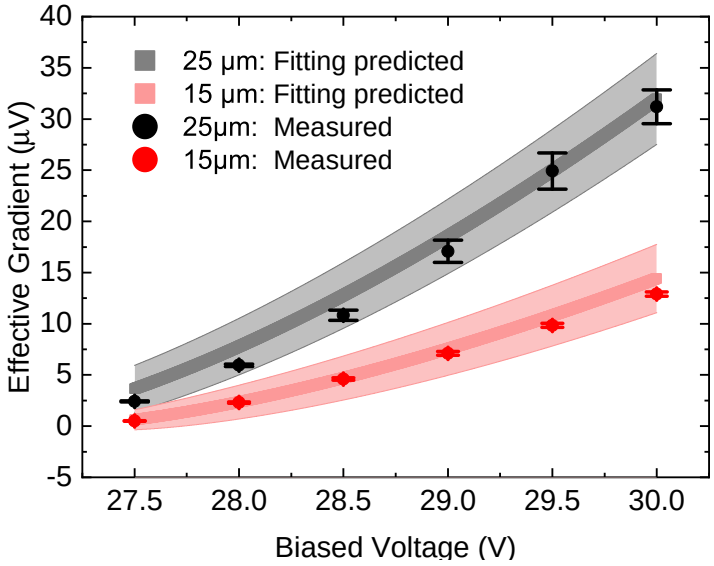

Figure 13: Linear region gradient as measured and as predicted by g and ϵ curves for the 2 KETEK chips. The shaded area is the standard error of the model, derived from the standard errors of the fittings in Fig. 12. The 'Measured' points are derived by fitting a straight line to the linear region of the response curve. The measured points lie close to the modelled regions using the g and ϵ fittings, confirming their validity.

here the linear region is more limited, and fewer points were available to perform the fitting.

In terms of the domain of linearity, the theoretical boundary on the linear region as predicted by Eq.4 and the fitted values for ϵ and g are shown on Fig.14. By inspection the region under the cut off is linear. It can be seen that both by increasing the number of micro cells and decreasing the biased voltage, the maximum of the linear domain can be extended.

6 511 keV Spectra

Having calibrated the SiPMs, a radioactive spectrum of ^{22}Na was obtained using the method described in Sec.3.1. The peak heights were binned, and where a peak appeared, a Gaussian function was fitted. The resolution of the detector was the full width half max of this fitting.

The output pulses of the two SiPMs with the LYSO were found to have a similar shape (Fig. 15). Comparing the traces from the two KETEK sensors to a similar SensL trace shows that the more expensive chip is faster. However the KETEK chips are comparable still in recovery time to the SensL one.

In terms of the energy resolution the two chips performed the same, with the 25μm cell size chip peaking at a value 3 times larger than the 15μm cell size chip at 30V bias voltage (Fig.16), consistent with the LED

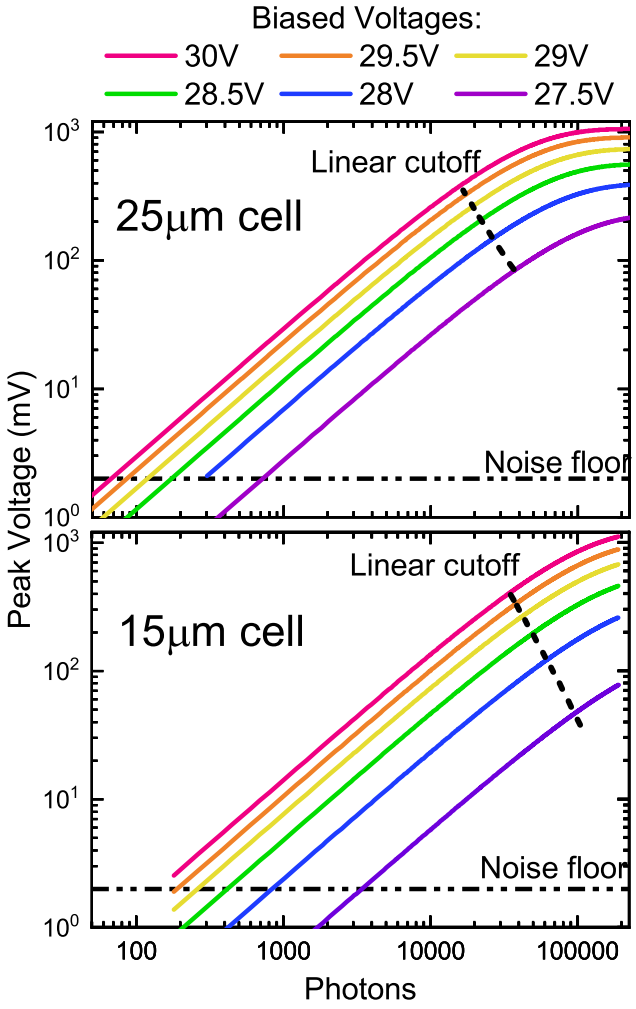

Figure 14: Fitting of the response curves of different biased voltages as indicated and plot of the number of photons below which the response is linear. Linearity defined as where the non-linear component of the fit contributes less than 10%. These 'cutoff' values are also indicated by vertical dashed lines on the plot on the left.

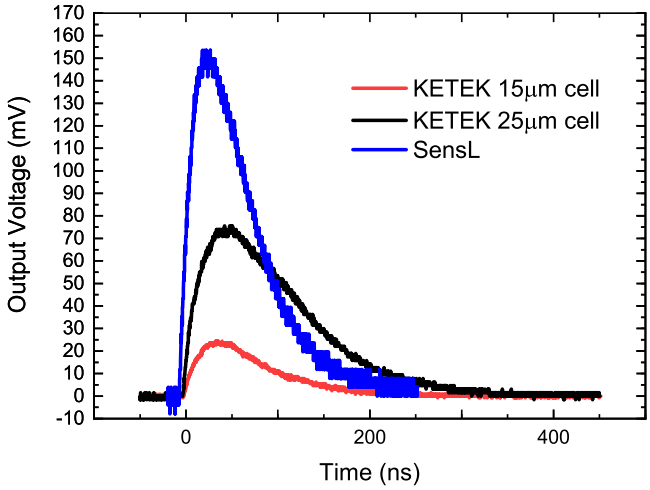

Figure 15: Typical trace from the KETEK SiPMs, cell sizes indicated. Peak height of traces illustrated are representative of a 511 keV LYSO detection. A similar output from the SensL chip is also shown. As can be seen, the SensL chip is much faster both in rise time and recovery than the KETEK ones. Biased voltage of 30V used, scope coupling at 50Ω

tests. The energy resolution of the 15μm cell size chip may be limited however by the digitisation noise of the scope, which was 1-2 mV. This is a significant fraction of the 24mV peak, and may contribute somewhat to the energy resolution.

The peak voltage at which the 511 keV line appears is indicated in the graphs. However the exact point this appears at was found to vary according to setup, with the coupling of the LYSO to the chip and the PTFE wrapping being difficult factors to control. Indeed if all the photons for a 511 keV x-ray absorbtion were detected the peak location is expected to be much higher. Further work is required to optimise light collection.

7 Amplification

In the tests carried out so far the response of the SiPM in the best case hit the noise floor of the picoscope at near 100 photons . This is inevitable given the fit parameters from Fig.12). At 30V, a g of 70μV means that a single cell firing produces a peak voltage of 70μV, far lower than the noise floor of the scope. Hence the effect of amplification of the signal was tested. The SiPM signal was passed through a Cremat CR-112 charge amplifier, which did increase the signal output. The floor for the number of detectable photons was lowered (Fig. 17), with the lowest detectable signal in the tens of photons. While this is not single photon level, this is a sizeable improvement. The amplifier does increase the noise of the signal, as can be seen in the larger error bars, but the effective increase of the noise floor does not counteract the lowered detectable signal.

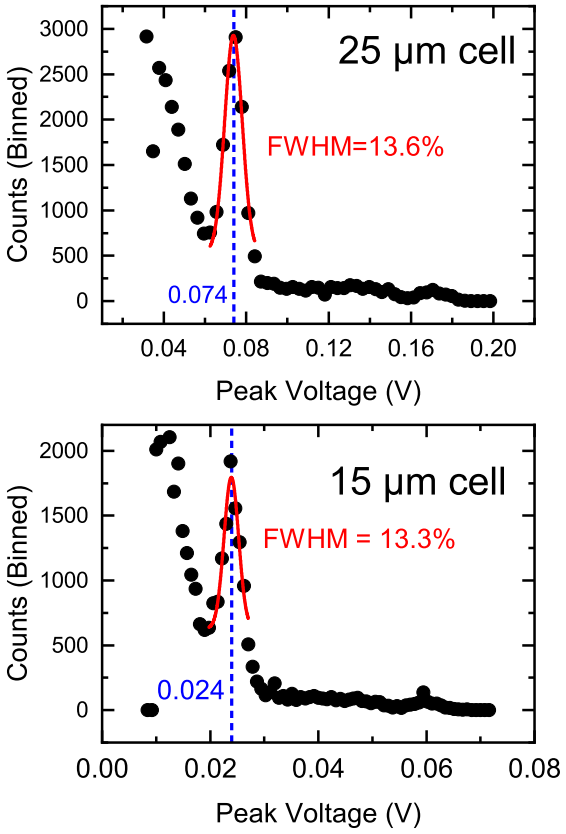

Figure 16: Spectra derived from binning of 5000 LYSO traces for both the tested SiPMs as indicated. The peak represents the 511 keV emission line of the ^{22}Na. The energy resolution of the two are comparable. Traces acquired at 30V biased voltage and 50Ω oscilloscope coupling

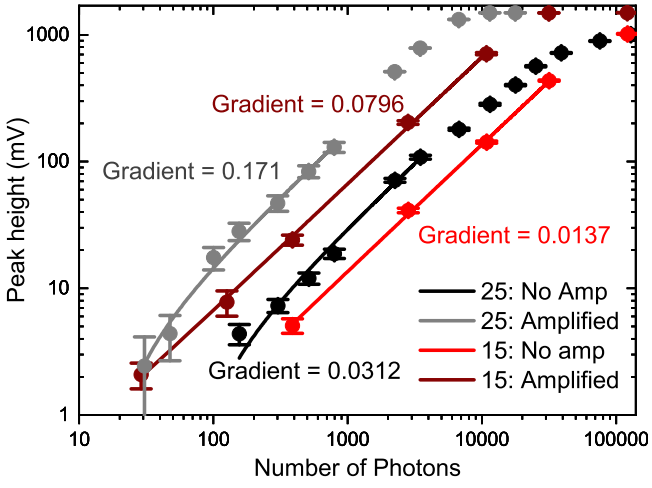

Figure 17: Response curve at 30V biased voltage for both the KETEK chips, with and without amplification. Amplifier used was a Cremat CR-112. The blue LED was used here, with the picoscope at 50Ω coupling

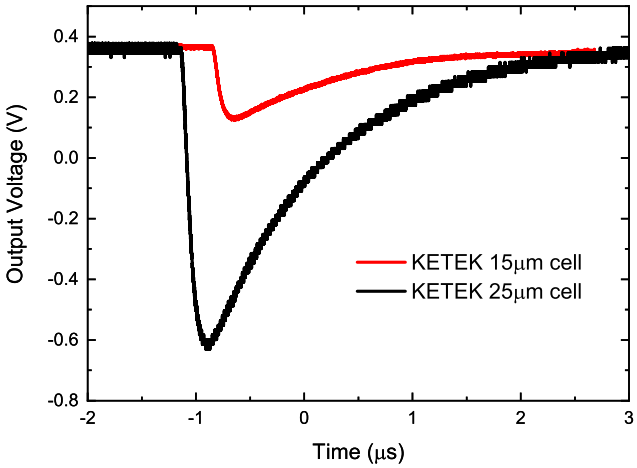

Figure 18: Typical LYSO trace for the two KETEK chips after amplification

A feature of the charge amp used is that it significantly increases the pulse length of the signal: The decay time is 50 μs [6]. While this makes the signal more susceptible to pile up, the added benefit is that fewer samples are required to digitise the output. The pulse length was found to increase significantly (Fig.18), moving into the micro second scale. For higher count rates the effect on the time resolution is significant, but for the count rates of this test this was not a problem.

Conducting the LYSO radiation test with the amplifier shows that the spectra from the 15μm cell size chip improves the energy resolution. The 25μm cell size chip does not show a significant improvement in energy resolution, but, there were more bins to fit a Gaussian function to. However, the peak lies very close to saturation level here, and higher energies will not be detected.

8 High count and Pile up

Finally the resolvability of 2 pulses was tested. At intensities similar to LYSO emission, the pile up effect was not a big problem with the 2 peaks smoothly merging into one. A separation of 50ns minimum was needed to resolve them as separate peaks (Fig. 20). The integral of the peaks did not change significantly.

8.1 High count rate with amplification

A spectrum was obtained using a high count rate Technetium source activity of 9.7 MBq, and the LYSO setup from Fig.6 was placed 15 mm from the source. The amplifier was used with a 25μm cell size chip for the detection. As seen in the previous section, before amplification pileup is not a significant problem. After amplification however, when the trace decay time is around 50μs, pileup of the amplified pulses is inevitable. still, it was found that as long as the pre amplified pulses are not

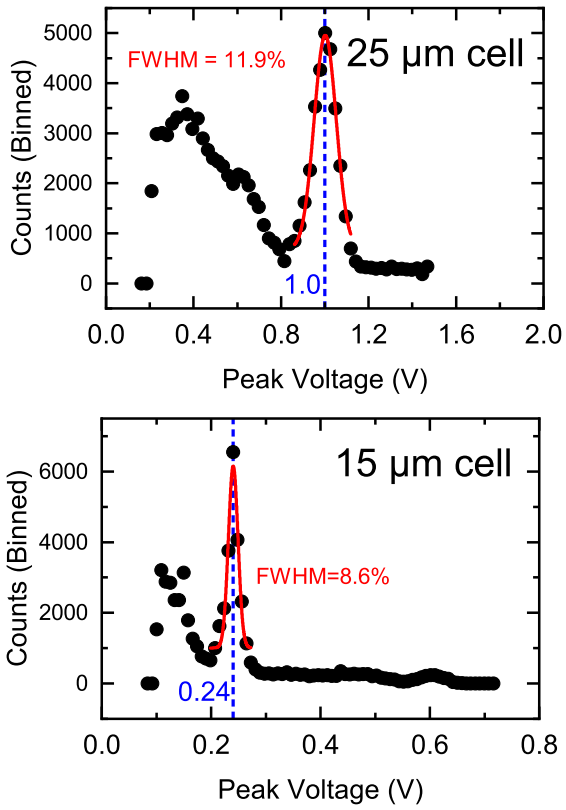

Figure 19: Spectra derived from binning of 5000 LYSO traces for both the tested SiPMs after amplification. The peak represents the 511 keV emissionline of the ^{22}Na.The 15μm celled chip shows greatly improved energy resolution. the 25μm chip has the peak very close to saturation. Traces acquired at 30V biased voltage and 50Ω oscilloscope coupling

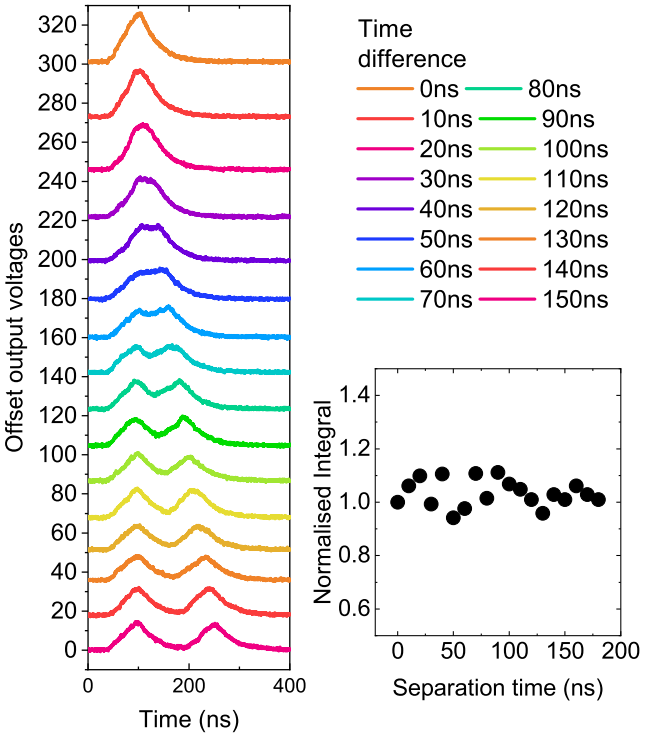

Figure 20: Two 68ns pulses from the blue LED separated in time as indicated. The pulse length and peak height of these were controlled to be similar to the LYSO trace in Fig.15, so as to simulate 2 LYSO emissions piling up. At separations less than 50ns, it becomes impossible to distinguish the two pulses.

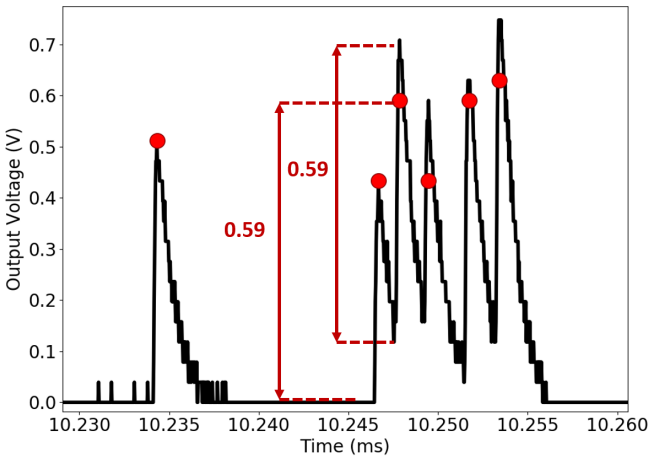

Figure 21: Trace of amplification pileup: Taken from a LYSO emission while exposed to a high count rate. Red dots mark the corrected height of the peak when the effect of pileup is removed. This test was done with DC coupling

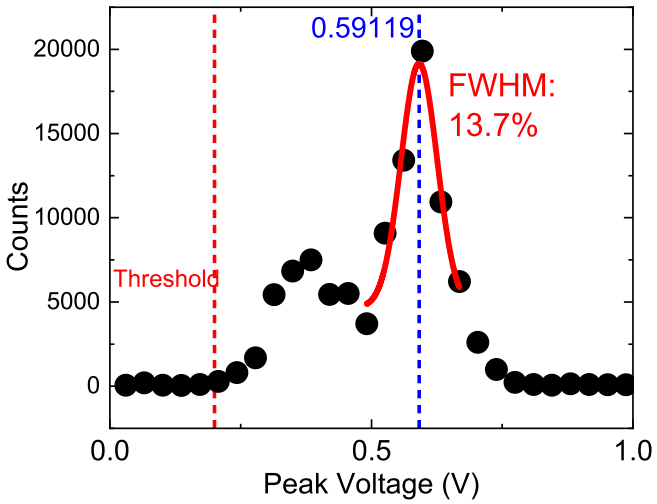

Figure 22: Spectra of activated Tc decay (emitting 141 keV X-ray) at 9.75 MBq. The Count rate is much higher, as seen by the peak height compared to the background

piling up, the information from the amplified pulse may be recovered (Fig.21). An analysis algorithm can easily be constructed to take this into account, as was done in this case.

The obtained spectra shows a peak that is far higher than the background (Fig.22).

9 Conclusion

The two KETEK chips compared through this report were found to be slower than the more expensive SensL chip, but not significantly enough to justify the price. Testing light response showed that for low intensities similar to typical scintillation emission, the 25μm cell size chip was more appropriate, as the smaller region of linearity was not a concern, but the added gain was a significant benefit. The biased voltage these operate at is recommended to be set high (30V being the highest tested) for the exact same reason. It was found that the energy resolution and the minimum floor of detectable photons is improved through an amplification of the signal. However for the 25μm cell size chip, this takes the 511 keV peak close to saturation, which may not be desirable. For an unamplified signal pile up was not a significant issue. The charge amplification was found to increase the pulse length to micro seconds, but the effect can be corrected for post amplification.

10 References

[1] KETEK GmbH. *Product Data Sheet: SiPM – Silicon Photomultiplier, PM3325-WB-D0* (2018).

[2] KETEK GmbH. *Product Data Sheet: SiPM – Silicon Photomultiplier, PM3315-WB-D0* (2018).

[3] SensL Technologies Ltd. *Introduction to SiPM: Technical note* (2011).

[4] Rusby, D. R. *Study of Electron Dynamics and Applications from High-Power Laser-Plasma Interactions.* Ph.D. thesis, University of Strathclyde (2017).

[5] Saint-Gobain Crystals. *Physical Properties of Common Inorganic Scintillators* (2018).

[6] Cremat Inc. *CR-112-R2.1 charge sensitive preamplifier: application guide* (2018).